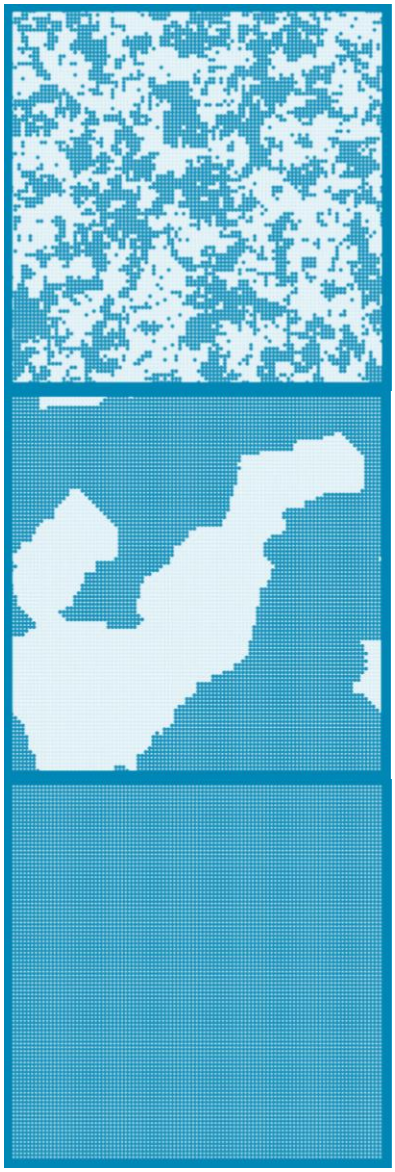

Using the Metropolis Algorithm to investigate the 2D Ising Model

ALEXANDRA MULHOLLAND
17336557

Prof Stephen Power | Computer Simulation | 10/11/19

Contents

1. Abstract

Computer simulating has been a crucial development in technology over recent decades, providing essential and applicable feedback on how we interpret real-world systems. One can portray and compare theoretical scenarios, and ones which are tedious to execute by hand. The purpose of this investigation was to simulate and investigate the 2D Ising Model by utilising the Metropolis algorithm. Variables such as the energy of the configuration, magnetisation, heat capacity and susceptibility were investigated relative to changing parameters such as temperature, number of iterations and magnetic field. This was carried out for a ferromagnetic material and anti-ferromagnetic material represented by a 10×10 lattice. Any larger lattices produced made for extremely long waiting times due to the nature of the computer system used. For the purposes of simplicity, the initial conditions were set as J (the exchange energy) being of constant value 1 and no external magnetic field. Thereafter, J was set as -1 to represent an antiferromagnetic material. The Curie and Néel temperatures were measured for each system and found to be $3.25K$ and $3.00K$ respectively. Additionally, snapshots of the configurations were produced at various values of the parameters for each system at a temperature below the critical. These accurately depicted the effectiveness of the algorithm in configuring the system to its optimal state. An animation was then prepared depicting a ferromagnetic material under no influence of an external magnetic field. This was accurately able to depict a lattice of any size as this was not under the restriction of computational power.

2. Scientific Background

Properties of magnetic materials

Due to the quantum mechanical angular momentum, or spin, of electrons, they harbour magnetic dipole moments, and so act as miniature magnets. This moment is described by equation (1), where $\boldsymbol{S}$ is the angular momentum of the electron, $\boldsymbol{\mu}$ is the magnetic dipole moment and γ is the gyromagnetic ratio, equal to $\frac{|e|g}{2m}$ for an electron (where g is known as the g-factor) [8].

$$\boldsymbol{\mu} = \gamma \boldsymbol{S} \tag{1}$$

Within the context of this investigation, we ascribe two quantum states: spin up or spin down, assigned 1 and -1 respectively. When subject to an external magnetic field, electrons will tend to align their dipole moments with the magnetic field as they experience a torque, described by equation (2) [8].

$$\boldsymbol{\tau} = \boldsymbol{\mu} \times \boldsymbol{B} \tag{2}$$

Whereby $\boldsymbol{B}$ is the applied external magnetic field. Paramagnetic materials are ones which exhibit a weak, but positive susceptibility to magnetic fields. This is due to the presence of a small number of unpaired electrons subject to torque. However, upon removal of the magnetic field, no magnetic property is retained, and the configuration of the material is one of randomly orientated spins with no net magnetic moment. A ferromagnetic material, however, as explained below, will have a large, positive susceptibility to magnetic fields, and retain a net magnetic moment upon removal of the external magnetic field [9].

Ferromagnetic and Antiferromagnetic Materials in the context of the Ising model

A ferromagnetic material is one whose spins are aligned parallel to each other, yielding an overall macroscopically sized magnetic moment. Let us first consider a 2-dimensional lattice of atoms which is under the influence of an externally applied magnetic field, h. The total energy of the overall configuration is written as in equation (3) below (the origin of said equation is explained in section -----). This equation is fundamental to the Ising model.

$$E[s] = -J \sum_{\langle i,j \rangle} \sigma_i \sigma_j - h \sum_i \sigma_i \tag{3}$$

J is the exchange energy, σ_i is the spin of a selected atom and σ_j is the spin of this atom's neighbours. The exchange energy is indicative of the influence of adjacent spins upon each other. Initially, the J value is set as a constant value and is equal to 1 and the external magnetic field is set as zero. This means the initial energy of the system is simply the sum of each atom's product with its neighbours. One may recognise that within a 2D lattice, each atom has 4 neighbours, therefore summing the spin-products will have a detrimental effect on the resultant energy, in that each atom's spin will be accounted for 4 times. Hence, one will observe in the code, the sum of the spin-products once the number of iterations has been attained is subsequently divided by 4. The term on the right, should there be an external magnetic field applied, will not have to be divided by 4, as no spin-products are being executed.

One can also infer from this equation that if the sum of the spin-product of a particle with its neighbours is negative, the resultant energy will be positive. Conversely, if the spins are aligned, the overall energy will be lowered. This can be explained via the Pauli-Exclusion principle, which dictates that electrons may not occupy the same quantum state. Demonstrably, when two adjacent particles are of parallel spins, they occupy the same orbital state, meaning they will be further from each other than those particles which have opposite spins. Consequence of the physical difference between them, the particles will experience different electrostatic energies. The J value measures this difference, as it is an indication of the coulombic interaction (i.e. its electrostatic origin) [3].
At positive J values, particularly those close to 1, the material is considered ferromagnetic, thus exhibiting a non-zero net magnetic moment. Here the exchange energy is at a minimum.
In the absence of an external magnetic field, a ferromagnetic material consists of many regions whereby a large number of atomic magnetic spins are aligned in parallel. These regions are known as domains, which are oriented in different directions and classified by strong exchange coupling of the individual microstates. Due to the random orientation of said domains, the material will exhibit a zero net magnetic moment. When a magnetic field is applied, these domains will align forming one single domain, thus the material will now exhibit a non-zero net magnetism [10] (this effect is illustrated in figure (1)) [11].
Here, the domain boundaries mark the separation of contrasting spins. The resulting torque from both the external magnetic field and the dipole moments of neighbours means the spins will be re-oriented to align with the magnetic field. Those domains whose spins are primarily aligned with the magnetic field will consequently grow. The effect of a larger external magnetic field is investigated within this computer simulation.

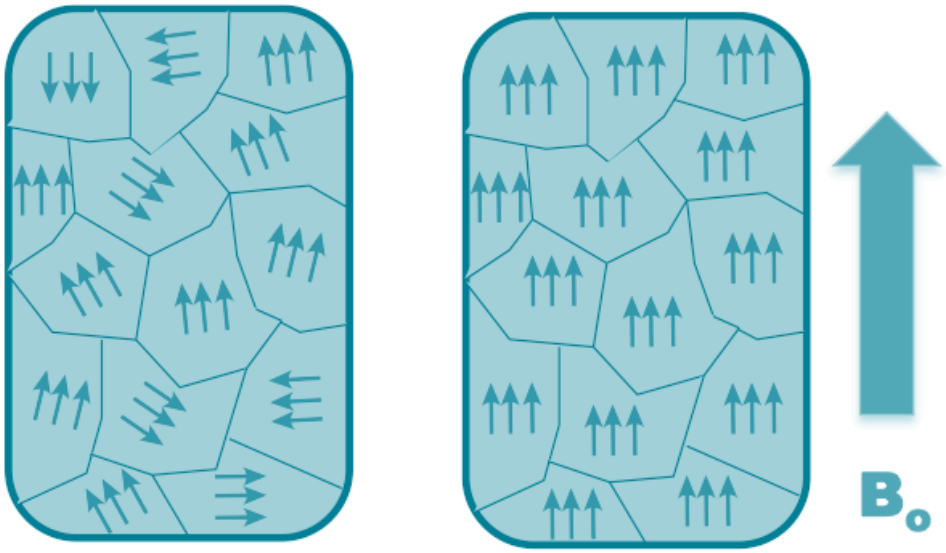

Figure 1: Diagram illustrating the effect of an external magnetic field, B_0, upon the domains of a ferromagnetic material

Antiferromagnetic materials exhibit antiparallel spins: here the J value is negative, and as such the material has a minimum exchange energy [5]. Antiferromagnetic materials demonstrate low magnetic susceptibility to any external magnetic field, as the antiparallel configuration is rigidly maintained even in the presence of this force. This arrangement ensues that the net magnetic moment will be zero. Figure (2) illustrates the difference between anti-, ferromagnetic and paramagnetic material structures.
One must note that this characteristics for ferromagnetic and antiferromagnetic materials are only observed at low temperatures. Above a certain temperature, these materials will demonstrate characteristics of paramagnets, explained in the following subsection.

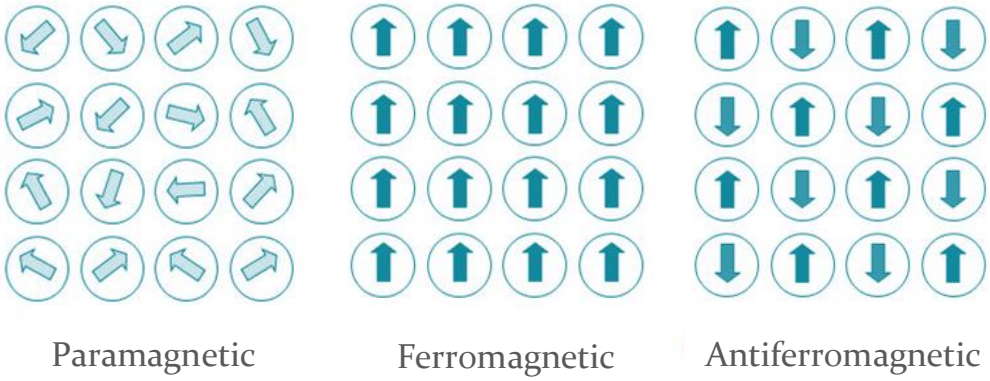

Figure 2: Simple diagrams illustrating the complexion of paramagnetic, ferromagnetic and antiferromagnetic materials. Here, the ferromagnetic material consists of one single domain after an external magnetic field has been applied.

The effect of temperature: The Curie and The Néel Temperature

It has been noted that the characteristics of ferromagnetic and antiferromagnetic are only exhibited at lower temperatures. At higher temperatures, however, these characteristics are unobservable. Let us first consider a ferromagnetic material: Above a certain temperature, known as the Curie temperature, the alignment within the domains is disrupted, and the material will become paramagnetic- meaning the domain structure and hence magnetic properties vanish. This transformation is known as a phase transition and is the result of thermal effects. The value of this temperature is unique to the ferromagnetic substance being analysed.
Analogous to the Curie temperature, the point at which a ferromagnetic substance will lose its anti-parallel alignment is known as the Néel temperature. The same thermal effect occurs here, and the substance will ultimately become paramagnetic. The value of said temperature is again intrinsic to the material being studied.
Both these temperature values, however, can be increased for a material by simply implementing a strong external magnetic field upon the material. This effect is investigated, presented and discussed in 'Results' and 'Discussion'.

Energy

Within this investigation, the change in the following variables were analysed against temperature and external magnetic field strength: The average energy, average magnetisation, the average heat capacity and the average magnetic susceptibility. The average energy of the system gives an indication of the equilibrium of the configuration. A lower energy value means the microstates have aligned in such a way that the microstate has reached its lowest energy state.

Equation 3 describes this parameter. This value will be negative as the configuration is effectively in a potential 'well', which will require energy (thermal) to remove it from this state. The lowest energy value will rise as the system undergoes a phase change from ferromagnetic to paramagnetic. Within this investigation, on will observe in the code that (as is all the variables) the average energy is calculated over a final number of steps and divided by the number of lattice points.

Magnetisation

This parameter expresses the density of a permanent or induced magnetic dipole. The magnetisation is calculated by summing the spins and dividing by the total number of lattice points, N^2. One can predict then, that for a configuration which is optimal, this value will be equal to 1 or -1. For the purposes of the plot, the magnetisation was plotted as an absolute value, thus will only result in a value of 1. At higher temperatures, the sum of the spins will not equal the number of lattice points: the configuration has been disrupted and the magnetization will most-likely less than 1 and greater than or possibly equal to zero (if the number of spins in the up direction is equal to those in the down direction). This would indicate the temperature is high enough for the material to reach complete 'disorder'.
Equation (4) describes an 'order parameter': the average magnetisation. This property will be zero in a "disordered" (paramagnetic or antiferromagnetic) state and either -1 or 1 in an ordered (ferromagnetic) state.

$$M_{av} = \frac{1}{N^2}\langle \sum \sigma_i \rangle \tag{4}$$

Susceptibility

The susceptibility of a material can be described as the derivative of the magnetization with respect to the externally applied magnetic field (5.i). From this, one will see that it can also be loosely described as the uncertainty in the magnetisation of the system squared, divided by the temperature. This is outlined in equation (5.ii).

$$\chi = \frac{dM}{dh} \tag{5.i}$$

$$\chi = \frac{(\Delta M)^2}{T} \tag{5.ii}$$

Figure (3) is demonstrative of the magnetic susceptibility trends one would expect for various materials with increasing temperature. [12]

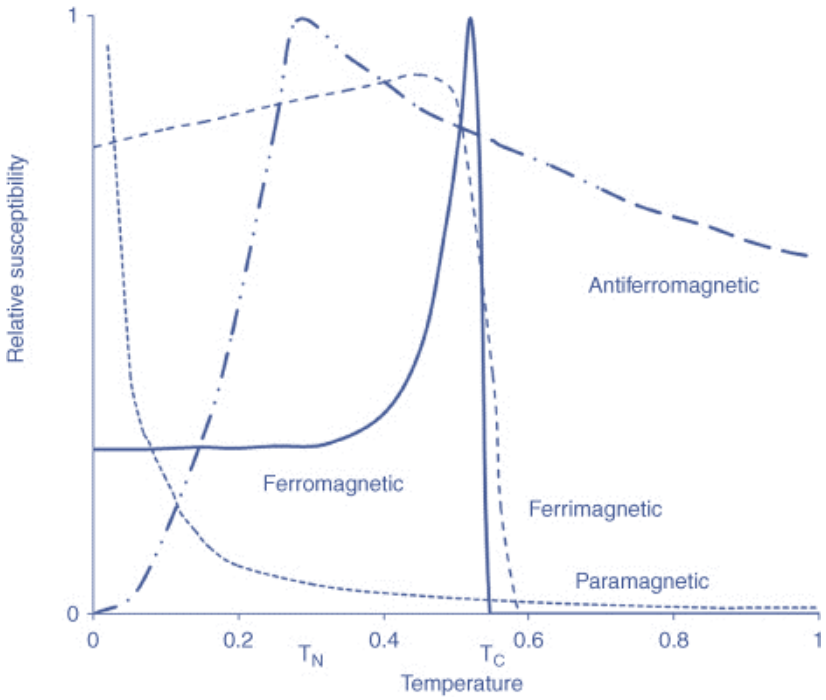

Figure 3: Plot demonstrating the change in magnetic susceptibility for paramagnetic, ferrimagnetic, ferromagnetic, antiferromagnetic materials with increasing temperature. The Néel temperature and Curie temperature are labelled as T_N and T_C respectively.

Heat capacity

Much like the magnetic susceptibility, the heat capacity of a material is the variance the average energy (or the error squared) divided by the temperature squared. This variable can be thought of as a material's capability to store energy. For a ferromagnetic material, this value will be at a peak value. The heat capacity of such a system is described by equation (6.i) below:

$$C = \frac{1}{T^2}(\langle E^2 \rangle - \langle E \rangle^2) \tag{6.i}$$

One should note that this formula, although it was used throughout the investigation, is not reflective of the true nature of the heat capacity. The correct formula is shown below (equation (6.ii)).

$$C = \beta^2(\langle E^2 \rangle - \langle E \rangle^2) \tag{6.ii}$$

Where β is $\frac{1}{k_B T}$, k_B being Boltzmann's constant. In the context of this model, Boltzmann's constant was taken to be equal to 1.

The 2D Ising Model

The Ising model is a mathematical model which, despite its simplicity in implementation, is rich in information which can be applied to numerous physical systems, such as alloys, 'lattice gases' and in this case, magnetic systems. Investigated by PhD student Ernest Ising in 1924, The Ising model was invented by Wilhelm Lenz in 1920, who presented this problem to Ising for the subject of his thesis. Although only investigated in one dimension, it was concluded that the model consisted of no phase transitions when representing ferromagnetism in any dimension [6]. However, as this paper will present, this is not the case.

The two-dimensional Ising model refers to a square lattice of atoms, with randomly assigned spins of 1 or -1, which interact only with their immediate neighbours. In this case, this entails 4 other atoms- 2 in the "vertical" direction and 2 in the "horizontal" direction.

As alluded to previously, the energy of an overall configuration i.e. the macrostate, is the sum of the individual microstates of the system. The energy function which describes this is known as the Hamiltonian, written as equation (3).

$$E[s] = -J \sum_{\langle i,j \rangle} \sigma_i \sigma_j - h \sum_i \sigma_i \tag{3}$$

Where each term has the same definition as in section 2.2. In this context, the external magnetic field, h, was made a positive constant, thus acting in the upward direction. The field will act on every particle, and so a sum over the total microstates must be taken to deduce its total contribution to the energy of the state [7]. One can see, that due to this negative sign preceding the terms, a ferromagnetic system will converge to a lower energy state as the configuration optimises: More spins will align resulting in an increase in the amount of positive spin products, thus, the negative sign multiplies to give a lower energy state.

To reiterate, in the neighbouring interaction term, the value of J dictates how strongly the neighbouring spins are coupled. The sign of this exchange energy is crucial in dictating if the material is ferromagnetic or antiferromagnetic.

The Metropolis Algorithm

The Monte Carlo Markov chain (MCMC) is a powerful numerical tool which can generate spin configurations and subsequently determine statistical averages and trends for such configurations. The Metropolis algorithm is an MCMC method which is used to acquire a sequence of random samples out of a distribution from which direct sampling is difficult and lugubrious. This method is advantageous in that it can accurately sample and draw conclusions for complicated distributions and high-dimensional spaces, even when regions of high probability are not easily located. However, in order to produce results of high accuracy, many samples are required. The main steps of the Metropolis algorithm within the context of this investigation are as follows (and represented as a flowchart in figure 3):

1. An initial configuration of spins is randomly generated within an N by N lattice.
2. A lattice point is chosen at random and its neighbours are identified.
3. The spin-product of the selected point and its neighbours is calculated
4. This product is multiplied by -2 (explained below) and is identified as the change in energy.
5. If this change in energy is greater than zero, the spin is flipped.
6. If not, the spin will be flipped with a probability of $e^{-\beta \Delta E}$
7. The new configuration has now been produced and the process is repeated for another randomly selected point of the lattice.

The main steps employed initially are ones reflecting a ferromagnetic material (for the system under no external magnetic field influence). Such a material exemplifies permanent magnetism due to the parallel orientation of the constituent spins.

The code used initially generates an N × N matrix of particles assigned their spins randomly. The Monte Carlo method then chooses a particle at random and compute the product of its spin with its four neighbours and sums these products. This sum of spin-products is multiplied by -2.

This is because the difference in the sum of spin-products calculated before and after the spin of the selected particle is flipped, is equal to twice the sum of spin-products of the original spin configuration. Later in the investigation, the effect of a magnetic field was considered. Here, there is a slight variation in the steps outlined above: the magnetic field strength is multiplied by the spin of the particle in question (the reason for this is clarified in the Scientific background section). This product is then multiplied by -2 analogously to the spin products: the change in the magnetic field-spin product will be double the initial product.

Naturally, the configuration will tend to a lower (more negative) energy, as otherwise the final configuration will not be permanent. The difference in energy is the initial energy subtracted from the final energy, and so for the spin flip to be carried out, the energy difference must be of a negative value. If this is the case, one can see in the code that the spin will then be flipped. In such a scenario, no work is required to flip the spin- in fact, energy will be released upon flipping the spin. However, if not, the spin is flipped with a probability equal to $e^{-\beta\Delta E}$ (the Boltzmann probability).

The code is set so that a final, optimum state is reached once a certain number of iterations via the Monte Carlo loop is executed. This state is one of minimum energy, whereby all the spins are parallel for a system which is ferromagnetic, or antiparallel for one which is anti-ferromagnetic. The complexion of ferromagnetic and anti-ferromagnetic materials has been discussed in detail in previous subsection 2.2.

3. Method and basics of implementation

The code was implemented on Jupyter Notebook, with Python being used as the programming language. For the purposes of simplicity, the Boltzmann constant was kept at a value of 1. Furthermore, through use of the modulo function, the boundary conditions were such that every particle within this N × N lattice had 4 neighbouring particles. The modulo function meant the square lattice was effectively a toroidal one, where the particles on the far-left edge were neighboured by those on the far right (the same applied for the top and bottom edges). The value of the exchange energy, J, was altered according to which type of material was being considered: ferro- ($J > 0$) or anti-ferromagnetic ($J < 0$). For both circumstances, each atom of the lattice was randomly designated a spin of 1 or -1. The Monte Carlo method was then implemented to reach an optimal configuration as appropriate for each material species. Here, as described previously, a point in the lattice is selected at random and if the energy change which would result (should the spin of said particle be flipped) is less than zero, then this particle is subsequently flipped. If not, the rand() function then generates a number between zero and 1. If the Boltzmann probability, $e^{-\beta\Delta E}$,(which one can see will always be greater than zero but less than one) is larger than the value generated, then the spin is flipped. If not, the spin remains the same. This procedure was looped over until the optimal configuration was attained. The grid size selected was 10 × 10, and so the number of iterations required to do so was chosen as around 1000, to ensure the expected system was obtained. The average values for energy, magnetisation, heat capacity and susceptibility were calculated over a certain final number of configurations. These variables were initially plotted against a temperature range in Kelvin, and subsequently plotted against a varying external magnetic field strength in Tesla (at a constant temperature). Certain magnetic field values were explored individually and examined by their effect on the variables' development with temperature parameter. Thereupon, snapshots of the configurations were plotted, whereby the culminated results were verified if they reflected the states of the ferromagnetic and antiferromagnetic materials.

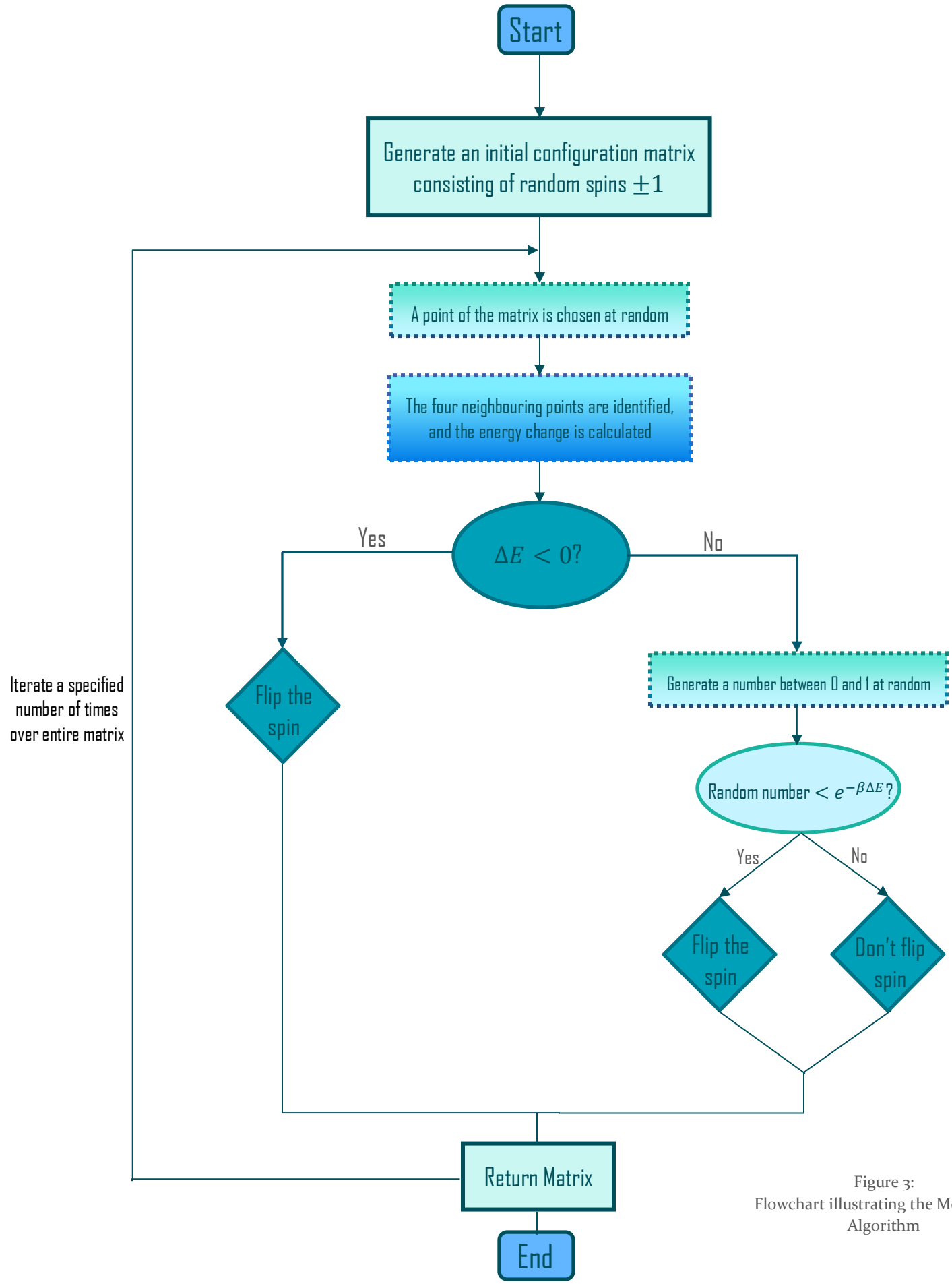

Figure 3:
Flowchart illustrating the Metropolis Algorithm

4. Results

This section is split into 3 parts corresponding to the three different codes:

- Part 1 illustrates the change of the parameters highlighted in 2.4 with increasing temperature. The exchange energy, J, was also varied to illustrate anti- and ferromagnetic materials. A constant external magnetic field was then applied, and the effects observed. (See part 1 code)
- Part 2 displays the change of said parameters with an increasing external magnetic field. J was varied as before and 2 temperatures either side of the Curie temperature (for ferromagnetic) and Néel temperature (for antiferromagnetic). (See part 2 code). A convergence test is also demonstrated via the magnetisation. (The code for said test, however, is contained within the part 3 code). See appendix for additional results.
- Part 3 of results contains the configuration plots for anti- and ferromagnetic materials at various points of the Metropolis Algorithm. (See part 3 code).
- Part 4 of the code executes an animation displaying the convergence of the configuration. (See part 4 code).

Part 1

Figures 1.1 to 1.4 show the variation in the investigated parameters for a temperature ranging from $0K$ to $10K$, with no influence from an external magnetic field.

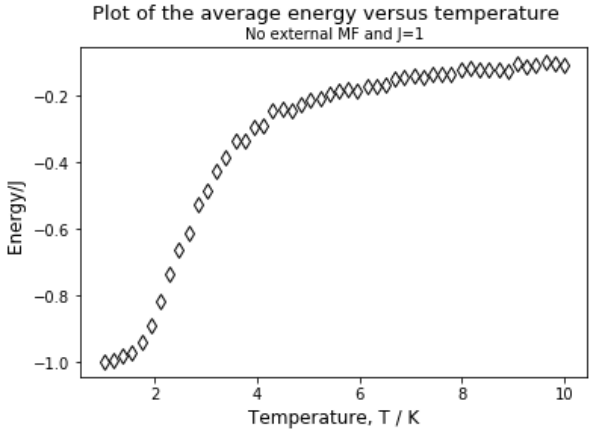

Figure 1.1: Plot of average energy versus temperature for a ferromagnetic material with zero external magnetic field

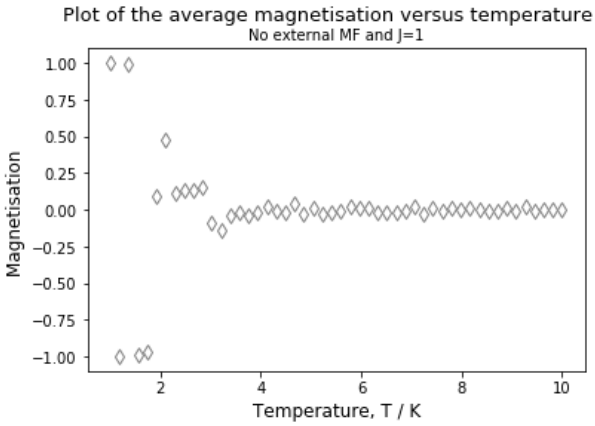

Figure 1.2: Plot of magnetisation versus temperature for a ferromagnetic material with zero external magnetic field

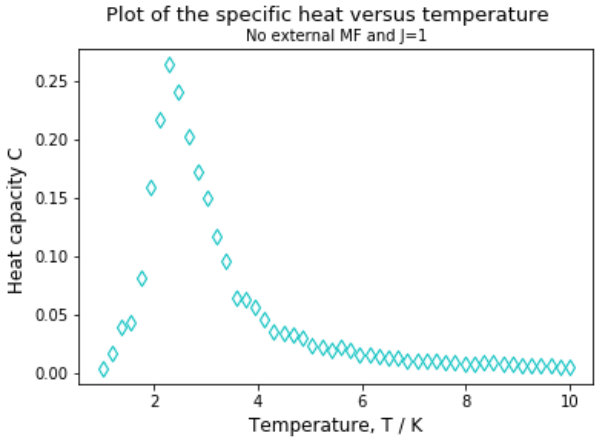

Figure 1.3: Plot of heat capacity versus temperature for a ferromagnetic material with zero external magnetic field

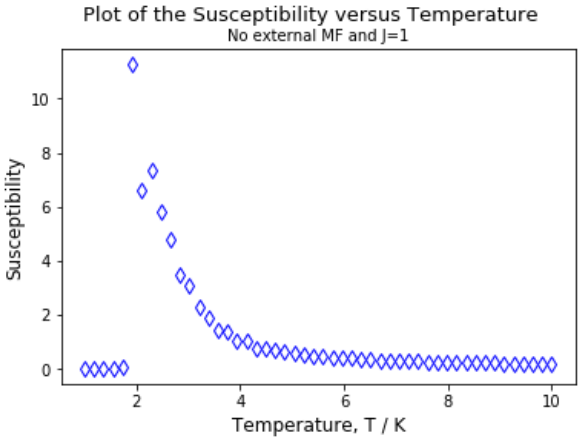

Figure 1.4: Plot of susceptibility versus temperature for a ferromagnetic material with zero external magnetic field

Figure 1.5 demonstrates the effect of an external magnetic field on the heat capacity of a ferromagnetic material.

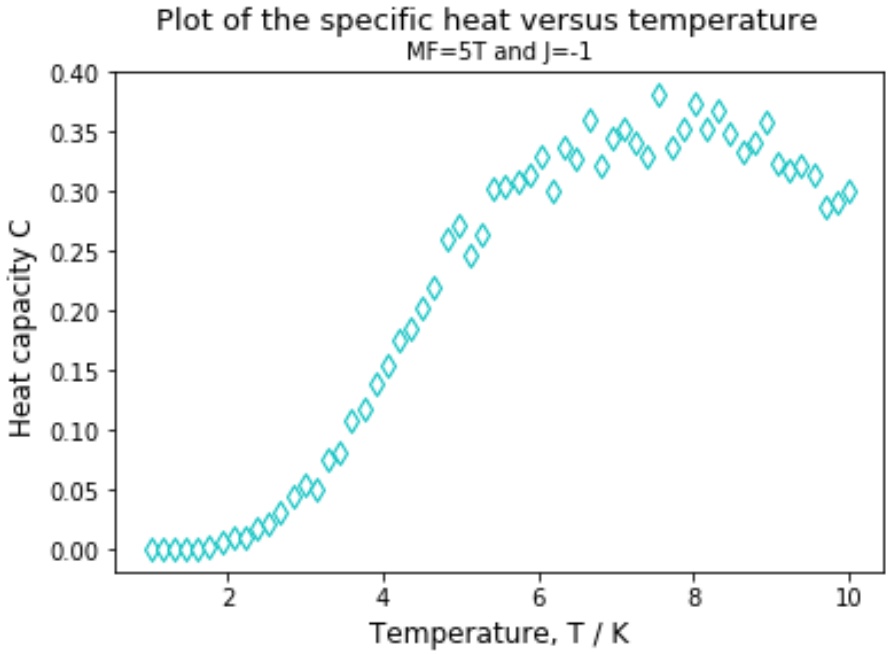

Figure 1.5: Plot of heat capacity versus temperature for a ferromagnetic material with an external magnetic field of 5.0T. (The title has been mislabelled as it should say J=1)

Figures 1.6 to 1.9 illustrate the same parameters changing with temperature (ranging from $0K$ to $10K$) for an antiferromagnetic material.

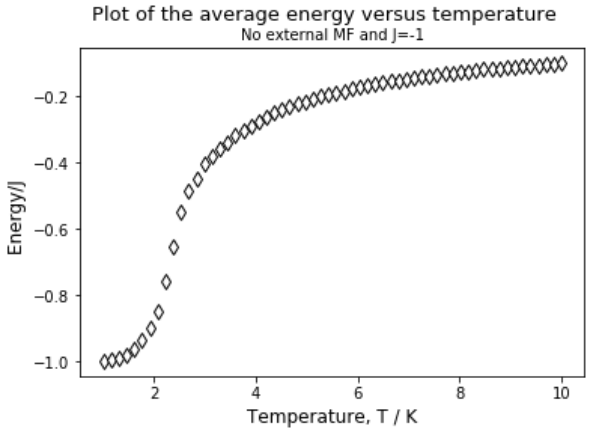

Figure 1.6: Plot of average energy versus temperature for an antiferromagnetic material with zero external magnetic field

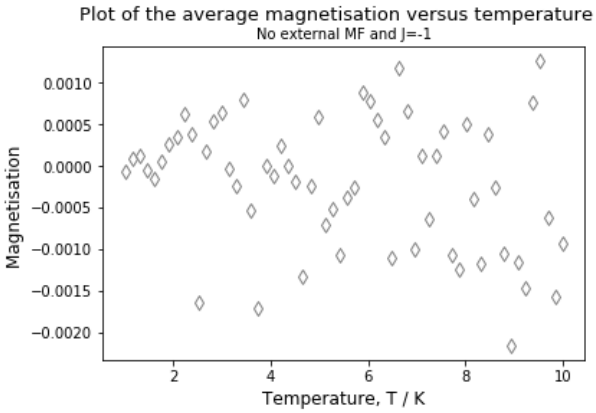

Figure 1.7: Plot of magnetisation versus temperature for an antiferromagnetic material with zero external magnetic field

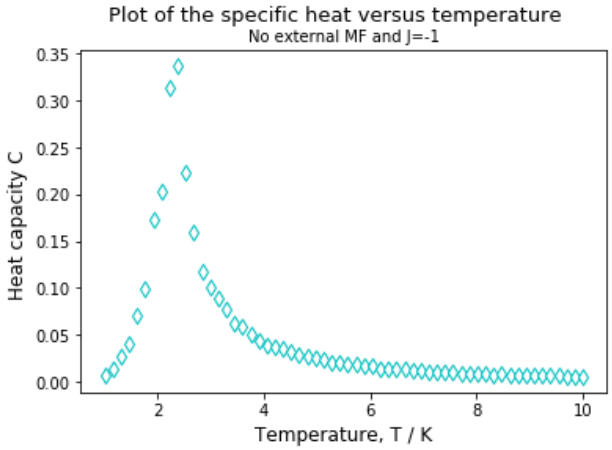

Figure 1.8: Plot of heat capacity versus temperature for an antiferromagnetic material with zero external magnetic field

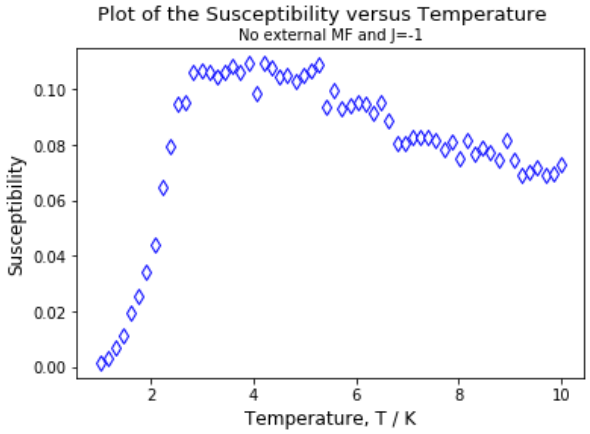

Figure 1.9: Plot of susceptibility versus temperature for an antiferromagnetic material with zero external magnetic field

Part 2

Figures 2.1 to 2.4 show the change in the four parameters with increasing external magnetic field strength at a constant temperature of 1K for a ferromagnetic material.

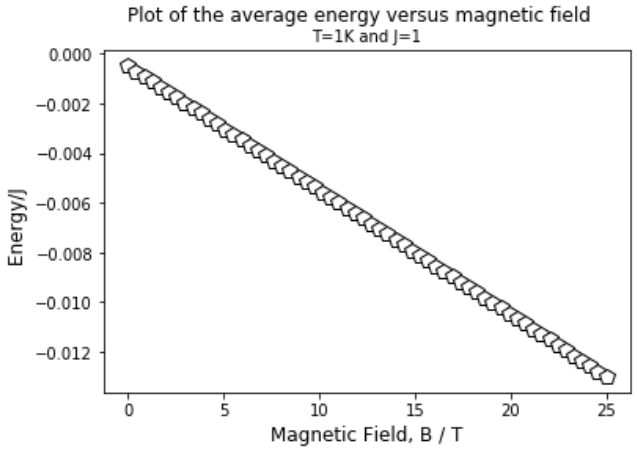

Figure 2.1: Plot of energy versus external magnetic field for a ferromagnetic material at a constant temperature of 1K (below the critical value)

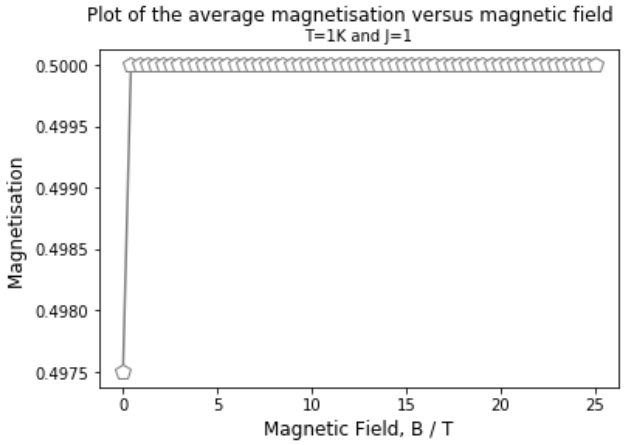

Figure 2.2: Plot of magnetisation versus external magnetic field for a ferromagnetic material at a constant temperature of 1K (below the critical value)

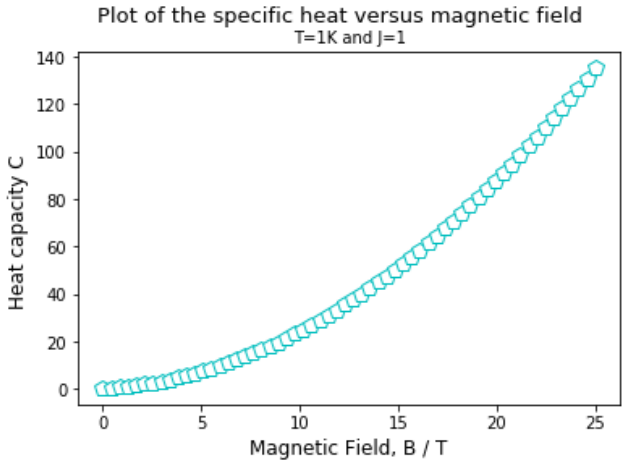

Figure 2.3: Plot of heat capacity versus external magnetic field for a ferromagnetic material at a constant temperature of 1K (below the critical value)

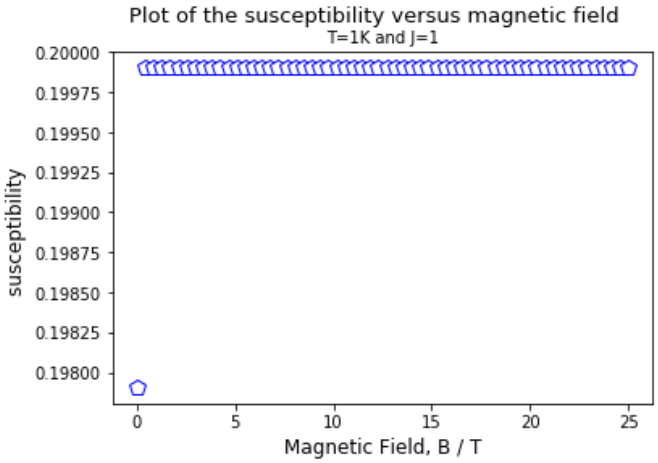

Figure 2.4: Plot of susceptibility versus external magnetic field for a ferromagnetic material at a constant temperature of 1K (below the critical value)

Figure 2.5 shows the effect of increasing the temperature to above the Curie temperature (to 5K) on the susceptibility.

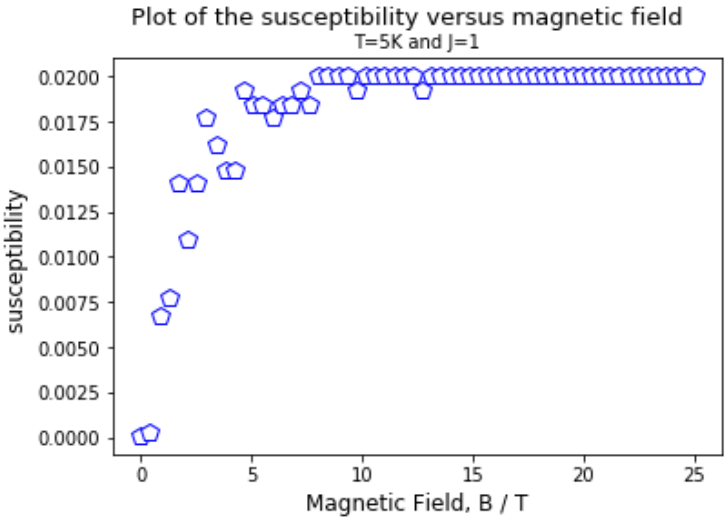

Figure 2.4: Plot of susceptibility versus external magnetic field for a ferromagnetic material at a constant temperature of 5K (above the critical value)

Figure 2.6 shows an indication of the convergence of the system in terms of total spin. This was executed for a ferromagnetic material (J=1) with no external magnetic field influence.

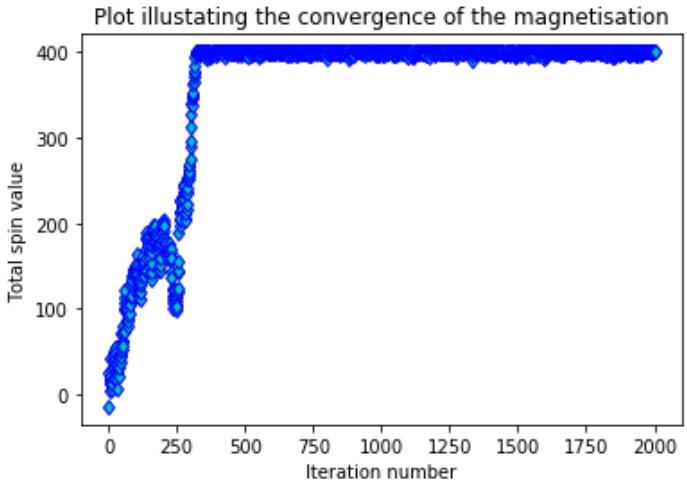

Figure 2.6: Plot of the total spin value against iterations for a ferromagnetic material with no external magnetic field.

Part 3

Figures 3.1 and 3.2 show configuration snapshots for a ferromagnetic (J was set to 1) and an antiferromagnetic material (J set to -1) respectively. Opposite spins are represented by different colours: green and blue.

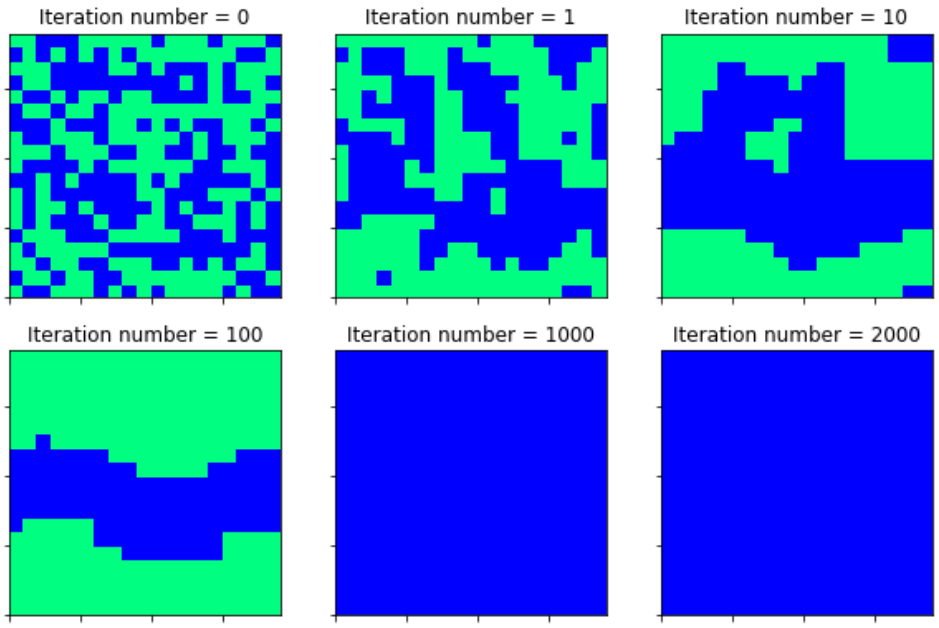

Figure 3.1: Configuration snapshots of the Metropolis algorithm for a ferromagnetic material.

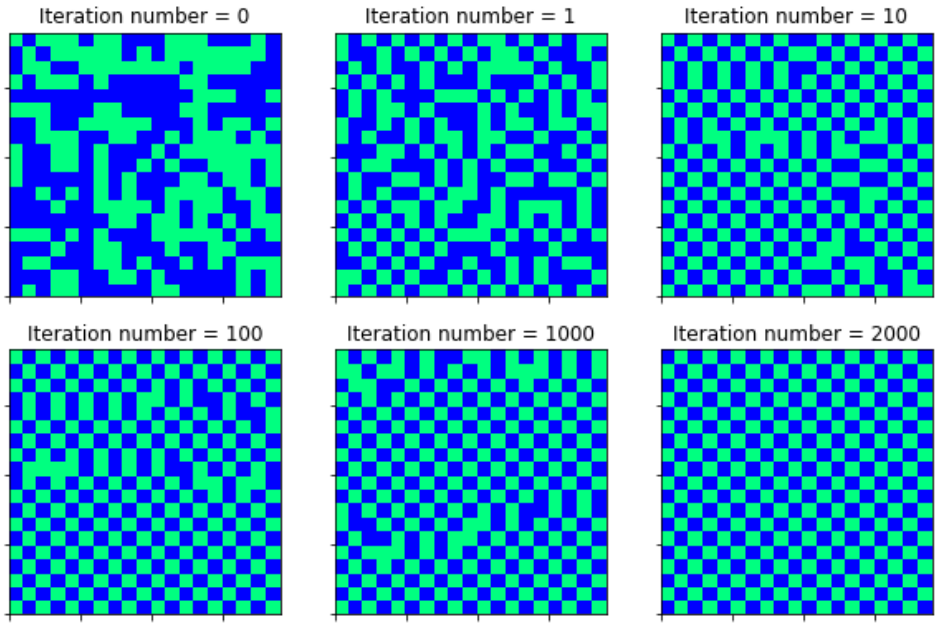

Figure 3.2: Configuration snapshots of the Metropolis algorithm for an antiferromagnetic material.

5. Discussion

Part 1

Figure 1.1 shows the average energy value of the ferromagnetic system as temperature increases. It represents a 10×10 lattice under no influence of an external magnetic field. The energy is described by equation 3, whereby the energy has been averaged over the final 'stepsmoncar' of the algorithm. Under no magnetic field influence, this equation becomes $E[s] = -J\sum_{\langle i,j\rangle}\sigma_i\sigma_j$. A J value of 1 and spin product value which will always be 1 upon equilibration ensures the minimum energy value for the material at $0K$ will be $-1J$. One can see that as the temperature rises, as does the energy value. This is indicative of the ferromagnetic material becoming increasingly disordered. From the graphs, the Curie temperature T_c appears to lie at approximately $3.5K$. As the temperature rises beyond this, the material becomes paramagnetic (one which demonstrates a complete disorder of spins). As a result, the energy values will be less negative than those when the material exhibited ferromagnetic properties.

Figure 1.2 shows the magnetisation versus temperature for the ferromagnetic system under the same conditions. Initially the configuration shows an expected value of either 1 or -1 for the magnetisation of a ferromagnet, as this is the sum of the total spin values divided by the number of spins. As the temperature increases, one can see the magnetisation begins to converge to zero. Around the Curie temperature ($3.0K$), the system has undergone a phase transition to paramagnetic. This means the sum of the spins will equal zero, as the spins throughout the lattice effectively cancel.

Figure 1.3 shows the change in heat capacity with temperature. We can see that this has a minimum value of approximately $0J/K$ at $0K$ and a maximum value at T_c. From this graph, it is difficult to identify which the exact critical temperature, however, an approximate value is at most $3.5K$. Beyond said temperature, the heat capacity exponentially decreases with temperature. This is evident from equation (6.i), where heat capacity has an inverse relationship with the square temperature. One can describe the heat capacity as the rate of change of energy with temperature. This highly evident from figure 1.1 where the steepest gradient occurs at the Curie temperature, and hence results in the highest value of the heat capacity at this point.

Figure 1.4 shows the change in magnetic susceptibility with increasing temperature. This parameter reaches a peak value of approximately 12 at around $2.2K$. Beyond which there is a steep decline until the critical temperature for a ferromagnet. From this graph, this appears to be around $3.0K$. The magnetic susceptibility, from equation (5.ii), is the variance in the magnetisation divided by the temperature, and so it is not unusual that the susceptibility is almost zero at low temperatures (where the uncertainty in the magnetisation is null). The peak value at around T_c is indicative of the thermodynamically complex nature of the system at this point, and so the uncertainty in the magnetisation will be significantly higher.

Figure 1.5 illustrates the hindering effect an external magnetic field exerts on a ferromagnetic system. Clearly the Curie temperature has become much more difficult to identify, such that it lies outside the boundaries of the scale. This is due to the magnetic field exerting a force on the lattice, encouraging the lattice to maintain order. Therefore, the phase transition to a paramagnetic material occurs at a much higher temperature.

Figure 1.6 plots the energy versus temperature for an antiferromagnetic material and appears similar to that of a ferromagnetic material. Again, from equation (3), and the fact that J=-1, one can see that the equation takes the same form as the equation rewritten above. Now, the spin product will be negative and so the ground state energy remains at -1 at $0K$. As the temperature increases, the material will undergo a phase transition to a paramagnetic material, analogous to the behaviour of a ferromagnet. In contrast, the critical temperature at which this phase transition occurs is known as the Néel temperature. Based on the graphs shown, this appears to occur at around $3K$.

Figure 1.7 shows the expected trend of the magnetisation for such a material, whereby beyond the critical temperature, the spins are disordered and result in larger, more varied magnetisation values. It appears this figure's scaling has been reduced by a factor of 1000. This may be due to the code, whereby the magnetisation was divided by the number of iterations (which was in this case 1000). Due to the total disorder of this graph, it is difficult to identify a Néel temperature.

Figure 1.8 shows the heat capacity versus the temperature for an antiferromagnetic material. Showing an almost identical trend to that of a ferromagnet, the critical temperature was identified to be around $3K$: consistent with previous trends and slightly higher the analytical result of around $2.3K$.

Figure 1.9 is a plot of the susceptibility of the antiferromagnet versus external magnetic field strength. To reiterate, susceptibility is effectively an indication of the error in the magnetisation. Therefore, this trend is as expected for low temperature values as below the critical point, the magnetisation will be that of an antiferromagnetic material: $+1$ or -1 and so the error in these values will be very low. As temperature increases, synonymous to a ferromagnet, the error in magnetisation and hence the susceptibility will increase and reach a maximum at the critical temperature ($3K$). Beyond this point, the material is now paramagnetic and so the error in magnetisation is much higher. The susceptibility steadily declines slowly but remains at a high value.

Part 2

Figure 2.1, while showing the expected trend of a linear slope downwards, does not show the expected values. The initial magnetic field strength at $B = 0T$ should have an energy of $-1J$ and decrease as the magnetic field strength increases in equation (3). However, it is initially zero. This is an anomaly which must be reviewed. Equation (3) accurately describes the trend whereby a linearly increasing magnetic field, at a temperature below the critical, will linearly decrease the energy of the system.

Figure 2.2 shows the magnetisation versus the magnetic field ranging from 0 to 25 Tesla, at a temperature of $1K$. This showed a constant value of 0.5. A configuration of spins will tend to align with the external magnetic field. Therefore, a constant value is logical as the configuration is already aligned upon configuration via the algorithm and so applying a magnetic field will have no further effect on the alignment. Figure 2.3 shows an exponentially increasing heat capacity with magnetic field. This is as expected as an increasing magnetic field encourages order to the system, and hence will induce a larger heat capacity.

Figure 2.4 shows a constant value for the susceptibility for an increasing magnetic field. This is as expected following the constant magnetisation value, as the error in this value will therefore be constant.

Figure 2.5 shows the influence of increasing the constant temperature to $5K$ on the susceptibility of the ferromagnetic system. One can see when comparing to figure 2.4, the system takes longer to reach a constant value. This is because the higher temperature encourages disorder (i.e. a paramagnetic system is observed). It appears this constant value is lower than that observed at $1K$ by a factor of 10

Figure 2.6 shows the convergence of the magnetisation for the system with increasing iterations in the Metropolis algorithm. This shows the expected trend whereby the total spin converges to a constant value of 400 upon optimal configuration. (In this case the size of the matrix was 20×20). This value in general will converge to a value of $\pm N^2$. This is an effective way of portraying the efficiency of the Monte Carlo method, whereby the optimal configuration was reached in under 500 iterations for this lattice.

Part 3

Figures 3.1 and 3.2 show snapshots of the configurations of ferromagnetic and antiferromagnetic systems respectively at various points in the Metropolis simulation. We can see that for a 20×20 matrix, the algorithm was carried out for 2000 iterations. However, as alluded to previously, this number of iterations is unnecessary as such an algorithm reached optimisation in under 500 iterations. The results for each are as expected: for a ferromagnetic material, the final configuration was all the same colour (i.e. all of the lattice points are of the same spin) and for an antiferromagnet, the final configuration resembles a chess board, representing every neighbouring point being of opposite spin.

6. Conclusion

Part 1 of the experiment showed the expected results for the energy, susceptibility, heat capacity and magnetisation for both a ferromagnet and antiferromagnet. When plotted against temperature, each property showed the expected trends: The energy for a ferromagnetic material had a ground state value of $-1J$, increased with increasing significantly upon the Curie temperature being reached, and flattened thereafter. The magnetisation showed an initial value of either 1 or -1 below the critical temperature, then converged to a value of zero upon the phase transition. The heat capacity, being the change in the energy with temperature, showed the expected trend, although the lack of expected sharp decrease in this trend made the Curie temperature more difficult to identify. This was also the case for the susceptibility: although showing the generally accepted trend, was perhaps in need of a larger sample size and a much larger number of iterations to display this value. From the ferromagnetic investigation, the Curie temperature was, on average, found to be around $3.25K$. This is close to the generally accepted value of $2.3K$ but perhaps a more effectively coded algorithm would result in a more accurate result. The effect of an applied magnetic field was represented well, whereby the Curie temperature was harder to identify on the heat capacity graph. Despite the slightly increased value of the Curie temperature, the code was able to accurately depict an antiferromagnet, with the Neel temperature found to be $3K$.

Part 2 of the investigation requires review. Unexpected values for energy and magnetisation and subsequently heat capacity and susceptibility were found when plotted against external magnetic field. This could be due to a small error in initialising the configuration and parameter values within the code. The convergence of the spin total was effectively produced, showing a result which converges to $N \times N$. The code for the configuration in part 3 accurately depicted both ferromagnets and antiferromagnets under the influence of no external magnetic field and at a temperature below critical.

Overall, the investigation was successful in depicting the behaviour of these parameters with temperature for both ferromagnetic and antiferromagnetic materials. The critical temperatures for both were identified and the results were similar, although slightly higher than the analytical result. Restrictions due to the processor in the computer used made it infeasible to plot larger configurations with more iterations. Upon re-evaluating these results, a higher computational power will be required. Furthermore, perhaps a triangular lattice could be investigated and to higher dimensions for a more representative view of the model. The 2D Ising model was simulated effectively using the Metropolis algorithm for a square lattice, despite the results requiring review.

7. References

[1] Darya Aleinikava
"The 2D Ising Model Monte Carlo Simulation Using the Metropolis Algorithm"
http://demonstrations.wolfram.com/The2DIsingModelMonteCarloSimulationUsingTheMetropolisAlgorit/
Wolfram Demonstrations Project
Published: August 30 2011

[2] Feynman, R. P.; Leighton, R. B.; and Sands, M. "Ferromagnetism." Ch. 36 in The Feynman Lectures on Physics, Vol. 2 Redwood City, CA: Addison-Wesley, 1989. 1996-2007 Eric W. Weisstein

[3] 1993, 1994, 1995, 1996, Nikos Drakos, Computer Based Learning Unit, University of Leeds.
[4] 1997, 1998, 1999, Ross Moore, Mathematics Department, Macquarie University, Sydney.

[5] Richard Boardman 2006-11-28

[6] K. Binder (2001) [1994], "Ising model", in Hazewinkel, Michiel (ed.), Encyclopedia of Mathematics, Springer Science+Business Media B.V. / Kluwer Academic Publishers

[7] jemdoc – light markup
Jacob Mattingley (www@jemnz.com)

[8] D.C. Giancoli, Physics for Scientists and Engineers, 3rd ed., page 1017. Or see: P.A. Tipler and R.A. Llewellyn, Modern Physics, 4th ed., page 309.

[9] NDT Education Resource Center, 2001-2014, The Collaboration for NDT Education, Iowa State University, www.ndt-ed.org.

[10] Ferromagnetic, paramagnetic and diamagnetic substances.
https://thefactfactor.com/facts/pure_science/physics/ferromagnetic/4702/

[11] Ferromagnetism - Questions and Answers in MRI, mriquestions.com/what-is-ferromagnetism.html 2019 AD Elster, ELSTER LLC

[12] Ferrimagnetism - an overview | ScienceDirect Topics. https://www.sciencedirect.com/topics/earth-and-planetary-sciences/ferrimagnetism